

NUMERICAL SIMULATION OF TURBULENT CHANNEL FLOW AT LOW PRANDTL NUMBER

By

K. Vasudeva Rao

ME14MTECH11008

Under the guidance of

Dr. K. Venkatasubbaiah

A Thesis Submitted to

Indian Institute of Technology Hyderabad

In Partial Fulfillment of the Requirements for

The Degree of Master of Technology



भारतीय प्रौद्योगिकी संस्थान हैदराबाद
Indian Institute of Technology Hyderabad

Department of Mechanical & Aerospace Engineering

IIT Hyderabad

July 2016

Declaration

I declare that this written submission represents my ideas in my own words, and where ideas or words of others have been included, I have adequately cited and referenced the original sources. I also declare that I have adhered to all principles of academic honesty and integrity and have not misrepresented or fabricated or falsified any idea/data/fact/source in my submission. I understand that any violation of the above will be a cause for disciplinary action by the Institute and can also evoke penal action from the sources that have thus not been properly cited, or from whom proper permission has not been taken when needed.

K. Vasudeva Rao

(Signature)

K. Vasudeva Rao

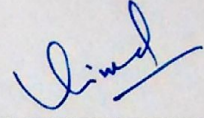
(Student Name)

ME14MTECH11008

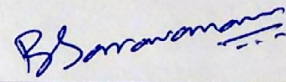
(Roll No.)

Approval Sheet

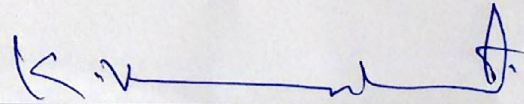
This Thesis entitled NUMERICAL SIMULATION OF TURBULENT CHANNEL FLOW AT LOW PRANDTL NUMBER by K. Vasudeva Rao is approved for the degree of Master of Technology from IIT Hyderabad



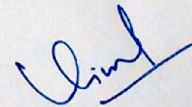
(Dr. Vinod Janardhanan) Examiner
Dept. of Chemical Engg.
IITH



(Dr. Saravanan Balusamy) Examiner
Dept. of Mechanical & Aerospace Engg.
IITH



(Dr. K. Venkatasubbaiah) Adviser
Dept. of Mechanical & Aerospace Engg.
IITH



(Dr. Vinod Janardhanan) Chairman
Dept. of Chemical Engg.
IITH

Acknowledgements

I would first like to thank my thesis advisor Dr.K.Venkatasubbaiah, Associate Professor at IIT Hyderabad. The door to my thesis advisor office was always open whenever I ran into a trouble spot or had a question about my research or writing. He consistently allowed this paper to be my own work, but steered me in the right direction whenever he thought I needed it.

I would also like to acknowledge Neelapu Satish,Ph.D student at IIT Hyderabad under the guidance of Dr.K.Venkatasubbaiah for his help in this thesis study.

Finally, I must express my very profound gratitude to my parents and to my friends for providing me with unfailing support and continuous encouragement throughout my years of study and through the process of researching and writing this thesis. This accomplishment would not have been possible without them. Thank you.

Abstract

Liquid metals are primary coolants in Generation IV nuclear reactors. For low Prandtl fluids, such as liquid metals, classical Reynolds analogy of using turbulent Prandtl number close to unity doesn't predict heat transfer characteristics correctly. In the present study turbulent forced convection flow in a channel at low Pr is studied numerically. Turbulence is modeled by Reynolds averaged Navier- Stokes (*RANS*) equations with low Reynolds number $k-\epsilon$ Launder sharma model. The governing equations are solved using high accuracy compact finite difference schemes with four stage Runge-Kutta method for time integration. Heat transfer characteristics of flow such as effect of Re , Pr on temperature and Nu are presented for different Reynolds and Prandtl numbers. A parametric study on variation of turbulent Prandtl number is done and using it comparing with the experimental Nu correlation, a new correlation has been developed for turbulent Prandtl number for low Pr flows. The present results are matching well with the experimental and numerical results available in the literature.

Contents

Declaration	ii
Approval Sheet	iii
Acknowledgements	iv
Abstract	v
Nomenclature	vii
1 Introduction	5
1.1 Literature Survey	7
1.2 Motivation	9
1.3 Objectives of Present study	9
1.4 Outline of thesis	9
2 Governing Equations (GE) and Boundary conditions(BC)	11
2.1 Dimensional form of GE	12
2.2 Boundary conditions and Initial condition	12
2.3 Stream function and Vorticity formulation	13
2.4 Non-dimensional form of GE	13
2.4.1 Non-dimensional variables	13
2.4.2 Governing Equations	14
2.5 Non-dimensional Boundary conditions and Initial Condition	15
3 Numerical methods	16
4 Results and Discussion	17
4.1 Grid independence and Validation	17
4.2 Effect of Reynolds number	19
4.3 Effect of Prandtl number	22
4.4 Effect of Turbulent Prandtl number	23
4.5 Nusselt number (Nu) calculation	25

4.6	Effect of Re on Nu	26
4.7	Effect of Pr on Nu	26
4.8	Effect of Pr_t on Nu	27
4.9	Correlation developed for Pr_t	28
5	Conclusions	30
	References	31

List of Figures

2.1	<i>Geometry of the Channel used for investigation</i>	11
4.1	<i>Grid independence for velocity and temperature profiles</i>	18
4.2	<i>U - grid independence</i>	18
4.3	<i>θ - grid independence</i>	18
4.4	<i>Validation of temperature profile in the channel with DNS and LES profiles</i>	19
4.5	<i>$Re=5600, Pr=0.01$</i>	19
4.6	<i>$Re=22000, Pr=0.01$</i>	19
4.7	<i>Contour plots of effect of Re on Velocity</i>	20
4.8	<i>Contour plots of effect of Re on temperature</i>	21
4.9	<i>Effect of Re on U</i>	22
4.10	<i>Effect of Re on θ</i>	22
4.11	<i>Effect of Re on velocity and temperature profiles</i>	22
4.12	<i>Effect of Pr on temperature</i>	23
4.13	<i>Contour plots of effect of Pr on temperature</i>	23
4.14	<i>Effect of Pr_t on temperature at a cross-section of channel</i>	24
4.15	<i>Contour plots of effect of Pr_t on temperature</i>	25

List of Tables

1.1	<i>Typical Pr for different fluids from Beitz and Kuttner</i>	6
3.1	<i>Numerical methods used for simulation</i>	16
4.1	<i>Effect of Re on Nu</i>	26
4.2	<i>Effect of Pr on Nu</i>	27
4.3	<i>Effect of Pr_t on Nu</i>	27
4.4	<i>Effect of Pr_t on Nu at Pr=0.01</i>	28
4.5	<i>Effect of Pr_t on Nu at Pr=0.025</i>	29

List of symbols

h	Width of the channel(m)
H	Convective heat transfer coefficient($\frac{W}{m^2K}$)
k	Turbulence kinetic energy (m^2/s^2)
k_n	Dimensionless turbulence kinetic energy
κ	Thermal conductivity ($\frac{W}{mK}$)
Nu	Nusselt number
Pr	Prandtl number
Pr_t	Turbulent Prandtl number
Re	Reynolds number
T	Temperature (K)
t	Time (s)
U_i	Inlet velocity (m/s)
u, v	Velocity components in x and y directions
U, V	Dimensionless velocity components in x and y directions
l	Length of the channel (m)
x, y	Cartesian co-ordinates
X, Y	Dimensionless scales in x and y directions
ψ	Stream function
ω	Vorticity
ϵ	Turbulence diffusion ($\frac{m^2}{s^3}$)
ν	Kinematic viscosity ($\frac{m^2}{s}$)
α	Thermal diffusivity ($\frac{m^2}{s}$)
ν_t	Turbulent eddy viscosity ($\frac{m^2}{s}$)
τ	Dimensionless time scale
θ	Dimensionless temperature
Ω	Dimensionless Vorticity
Ψ	Dimensionless stream function
ϵ_n	Dimensionless dissipation

p Pressure(Pa)
 c_p Specific heat at constant pressure ($\frac{J}{kg \cdot K}$)
 Pe Peclet number

Chapter 1

Introduction

Liquid metals are used in many nuclear and non-nuclear processes associated with thermal hydraulic aspects. In the nuclear field liquid metals are used in fission and fusion reactors. In the nuclear fusion reactor the use of liquid metals is broader. In the fast breed reactor sodium is used as a coolant while in new breeder concepts often lead or lead alloys are used. A study regarding type of coolant and their advantages and disadvantages were given in David^[1] for nuclear reactors. In non-nuclear applications also liquid metals are used as heat exchange medium. For example in solar plants heat ex-changers that are operating with liquid metals (see Benemann^[2]). In manufacturing industries such as refinery and casting of metals as well as glasses behavior in molten condition is similar to liquid metals, the same heat transfer problem appear as in nuclear field power generation applications.

In Nuclear Power plant engineering, *OECD* (Organization for Economic Cooperation and Development) and *NEA* (Nuclear Energy Agency)^[3] nuclear science committee proposed different suggestions or improvements that can be made to increase the efficiency of power plant. Out of these improvements use of Gen IV Nuclear reactor is one of the important one. In this Gen IV reactor the main feature is use of Liquid metal as a primary coolant instead of water.

The two important different properties of any metal from other media are high thermal conductivity(κ) and low specific heat capacity(C_p). In case of heavy liquid metals the kinematic diffusivity is also less compare to that of air or water. The non-dimensional number covering thermal conductivity and specific heat capacity is Prandtl number (Pr). The physical sense of this number is the ratio of momentum diffusivity to thermal diffusivity. For liquid metals this number is very low since the thermal diffusivity is high compared to momentum diffusivity. Thus liquid metals can carry more thermal energy with them and

hence it increases the efficiency of the power plant. The Prandtl number for these fluids is generally around 0.01. The peculiarity of such low Prandtl fluids is that for moderate Reynolds number flows even though the flow is fully turbulent the temperature profile is smooth and is more of a laminar flow behavior.

The Prandtl number values for different fluids are given in Table 1.1. More details can be found in Beitz and Kuttner^[4]. In this table we can see order of Prandtl number for fluids like engine oil is $O(10^3)$ and for fluids like air and water is $O(1)$ and for liquid metals it is $O(10^{-2})$.

Table 1.1: Typical Pr for different fluids from Beitz and Kuttner

Temperature(C)	Mercury	Air	Water	Engine oil
0	0.0288	0.72	13.6	$4.7 \cdot 10^4$
20	0.0249	0.71	7.02	$1.0 \cdot 10^4$
100	0.0162	0.70	1.74	$2.6 \cdot 10^2$

In general all the fluid flows can be categorized into three groups, i.e. $Pr \ll 1, Pr \gg 1, Pr \approx 1$. In case of forced convection systems under laminar flow conditions the Prandtl number covers the thermal energy transfer part for all types of fluids mentioned above. In turbulent flow in addition to molecular conductivity eddy conductivity is also important. The order of these conductivities are also of same range. In case of air or water ($Pr \approx 1$) or high Prandtl fluids like engine oil ($Pr \gg 1$) the thermal effects are close to viscous sub layer, but for liquid metals ($Pr \ll 1$) the thermal effects are much towards the core of turbulent flow. Therefore, the fundamental details of heat transfer mechanism in liquid metals differ from that of air or other Newtonian fluids and hence the heat transfer correlations used for air or other fluids can't be used for liquid metals.

There are several experimental studies^{[5][6][7][8]} in this field of low Prandtl number fluids, but there are some difficulties in experiments such as non-wetting of the fluid with the solid used at the interface, oxidation of liquid metal with the solid at the interface. Gases are also entrapped due to non-wetting. Hence due to these impurities the heat transfer is less than the actual heat transfer and hence the experimental results differ from numerical results but still care has to be taken while performing the experiment. Thus the numerical simulation is an important tool in design when compared to experiments. In the numerical simulations *RANS* (Reynolds Averaged Navier Stokes) approach is widely used for less cost and time compared to *DNS* (Direct Numerical Simulation) or *LES* (Large Eddy Simulation) ap-

proaches. In *RANS* approach for $Pr \approx 1$ constant turbulent Prandtl number (Pr_t) equal to unity is used. Turbulent Prandtl number (Pr_t) signifies the ratio of eddy momentum diffusivity to eddy thermal diffusivity. For liquid metals constant Pr_t close to unity can't be used since the eddy thermal diffusivity and eddy momentum diffusivity are of no same order.

1.1 Literature Survey

Research on the use of low Prandtl fluid in channel at turbulent flow conditions has been done considerably in previous literature. Hiroshi Kawamura^[9] has done Direct Numerical Simulation (*DNS*) of channel flow at friction Reynolds number (Re_τ) equal to 180 for a wide range of Prandtl numbers (Pr) and concluded that turbulent Prandtl number (Pr_t) is dependent on Pr for $Pr < 0.1$. Again Hiroshi Kawamura^[10] has done *DNS* simulations of channel flow at Re_τ equal to 180,395 at Prandtl numbers 0.025,0.2 and 0.71 and presented the effects of Reynolds number(Re), Prandtl number(Pr) on temperature. Reynolds^[11] reviewed and assessed more than 30 studies in the open literature on turbulent Prandtl number and divided them into several groups according to their approaches, i.e. from highly analytical derivation to purely empirical methods. It was pointed out that empirical models show clearly higher accuracy, although the highly analytical models imply more phenomenological understandings. Hence for practical application, empirical models are still preferred. Out of different empirical models in the literature Cheng and Tak^[12] has done a review on models proposed by Aoki^[13], Reynolds^[11], Dwyer^[14] for circular tubes. Out of these models Aoki^[13] model predicts higher values than other models. Dwyer^[14] model predicts less value compared to other models. The first heat transfer theory specifically applicable to liquid metals was proposed by Martinelli^[15]. He applied the analogy theory of turbulent momentum and energy transfer to liquid metals taking into account molecular thermal conduction. With this theory, Lyon^[16] derived a semi-empirical equation for calculating heat transfer in liquid metals for the case of constant heat flux. Dwyer^[14] applied his correlation of turbulent Prandtl number to the heat transfer equation developed by Lyon^[16] and proposed a new correlation for Nusselt number for liquid metals with constant heat flux as boundary condition. Later Skupinski et al^[7] proposed a correlation for Nusselt number based on the experimental heat transfer in *NaK* (Sodium potassium) liquid metal flows. Sleicher et al.^[6] conducted experiments with *NaK* flows at boundary conditions of both uniform wall temperature and uniform heat flux and concluded that heat transfer coefficients in case with uniform heat flux are higher compared

to case of uniform wall temperature. Based on experimental results he proposed a correlation for Nu in liquid metal flows. Stromquist^[8] has done experiments on mercury flows and proposed a correlation for Nu . Ibragimov et.al.^[17] conducted experiments with Lead bismuth eutectic alloy (LBE) flows and proposed a correlation. This correlation gives best result for the wall temperatures measurement in liquid metal flows. Based on experimental data of NaK , Lead, LBE , mercury flows Kirillov^[5] discovered that there exists large discrepancies in the experimental data with different fluids but all were lower than the values obtained by $Pr_t=1$. Later Kirillov and Ushakov^[18] proposed a correlation for Nu for LBE flows. Cheng and Tak^[12] has done a review on the existing correlations. Since there are no complete and consistent experimental data available in open literature except that of Johnson et al^[19] he selected it for the assessment of heat transfer correlations available in the literature. The correlation of Lyon^[16] with $Pr_t=1$ gives higher heat transfer co-efficients when compared to other correlations where as by using higher turbulent Prandtl number($Pr_t=3$) it agrees on the average well with the experimental data. The correlations developed using NaK experimental data^{[7],[6]} gives higher heat transfer correlations than the other correlations proposed for LBE ^[17] and mercury flows^[8]. In the low Peclet number region, both correlations of Kirillov^[18] and Ibragimov^[17] show a better heat transfer than the correlation of Stromquist^[8], where as at high Peclet number, the Stromquist^[8] correlation predicts a higher heat transfer coefficient than the correlation of Ibragimov^[17]. With Johnson's^[19] experimental data he found that at low Peclet numbers Kirillov's^[18] correlation gives the best agreement with the experimental data and at high Peclet numbers Stromquist^[8] shows the best prediction. Using this Cheng and Tak^[12] proposed a correlation for Nu for LBE flows. He has also explained possible reasons for the discrepancies in the correlations present in literature. They are missing on reliable test data, thermal contact resistance, surface wetting, local detachment and buoyancy effects. Kirillov^[20] and Subbotin et al.^[21] analyzed heat transfer experimental data in heavy liquid metal (HLM) flows using two different approaches to obtain the temperature on the heat transfer surface. One is by extrapolating from the temperature profile of flow and other is by direct measurement. They found that due to thermal contact resistance the extrapolated temperature is less than the measured wall temperature. Tim Abram and Sue Ion^[22] has done a review of state of science in nuclear power and stated that the five systems are selected for the development of reactor in nuclear field. Out of the five systems, Lead Fast reactor (LFR) and Molten Salt reactor (MSR) are examples of low Prandtl fluid systems. Bricteux et.al^[23] has done DNS and LES of channel flow at Re_τ equal to 180, 590 at Prandtl number 0.01 and concluded that turbulent Prandtl number should be used with care in $RANS$ approach. Kays^[24] proposed a correlation for turbulent Prandtl number for

RANS approach. Duponcheel.et.al^[25] has done *DNS* and *LES* of turbulent channel flow at Reynolds number equal to 5600, 22000, 24000,87000 for Prandtl number range 0.01 to 0.025 and compared it with the *RANS* approach and stated that kays correlation for turbulent Prandtl number is most suited for *RANS* approach.

1.2 Motivation

Studies in the past have not emphasized the effect of turbulent Prandtl number in forced convection channel flow at low Prandtl number using *RANS* approach. The constant turbulent Prandtl number obtained from different correlations have discrepancies. A detailed flow characteristics for variation of Pr_t and effective turbulent Prandtl number for channel flow at low Prandtl number is also not presented in the literature. This is the motivation for the present study.

1.3 Objectives of Present study

The main objective of present study is to study the behavior of turbulent forced convection in channel flow with low Prandtl number fluids. They include velocity and heat transfer characteristics. The important objectives are

- To study the effect of Reynolds number (Re) and Prandtl number (Pr) on the flow behavior. (Combined effect is effect of Peclet number ($Pe = Re * Pr$.)
- To study the effect of turbulent Prandtl number (Pr_t) on the flow behavior.
- To study the Nusselt number variation with respect to different Re, Pr, Pr_t .
- A parametric study of Pr_t on thermal characteristics of the flow.

1.4 Outline of thesis

Numerical simulation of turbulent channel flow at low Prandtl number.

- Chapter 1: In this chapter introduction about the turbulent channel flow using low Prandtl number fluids is presented. In addition literature survey, motivation to take this as thesis study and also objectives of present study are also presented.
- Chapter 2: In this chapter governing equation of two dimensional incompressible forced convection flow through channel in dimensional and non-dimensional form and corresponding boundary conditions are also presented.
- Chapter 3: In this chapter numerical methods used to solve the governing equations are presented.
- Chapter 4: In this chapter the results that are obtained are discussed and presented.

Chapter 2

Governing Equations (GE) and Boundary conditions(BC)

The problem statement is turbulent forced convection in a channel and it can be seen in Fig.2.1. It is solved using Reynolds Averaged Navier Stokes (*RANS*) equations. Reynolds time averaging is suitable for stationary turbulence. In this analysis at any instant of time flow variable can be expressed as the sum of mean and fluctuating quantities. The turbulence closure problem is solved by using standard $k-\epsilon$ equations. As this is a two dimensional problem stream function and vorticity approach is used to solve the equations. Advantages of this formulation are added accuracy due to exact satisfaction of mass conservation and reduction in the number of unknowns to two as compared to three unknowns for primitive variable formulation. Pressure is eliminated by taking the curl of the momentum equation to give the vorticity transport equation (*VTE*).

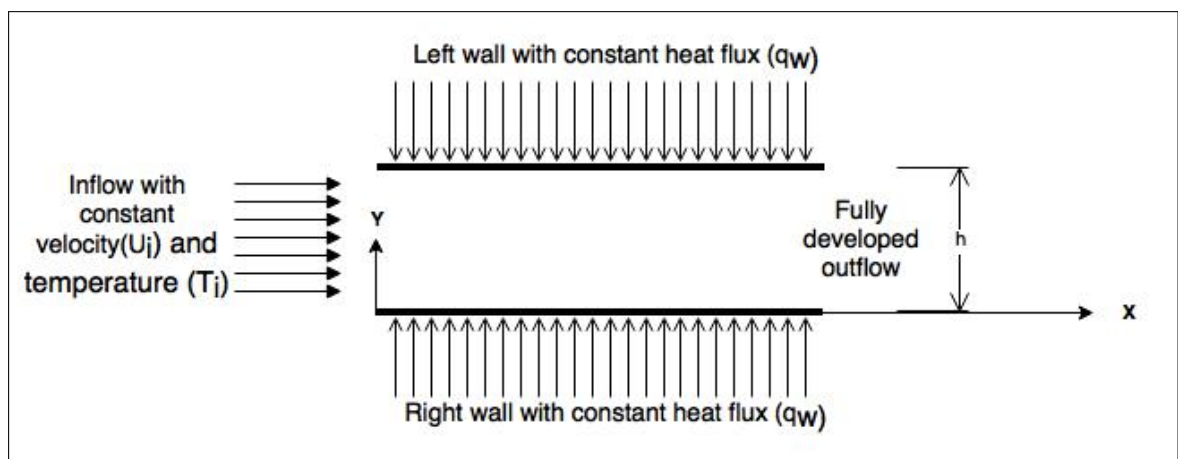


Figure 2.1: *Geometry of the Channel used for investigation*

2.1 Dimensional form of GE

$$\frac{\partial u}{\partial x} + \frac{\partial v}{\partial y} = 0 \quad (2.1)$$

$$\begin{aligned} \frac{\partial u}{\partial t} + u \frac{\partial u}{\partial x} + v \frac{\partial u}{\partial y} = & -\frac{1}{\rho} \frac{\partial p}{\partial x} + \nu \left(\frac{\partial^2 u}{\partial x^2} + \frac{\partial^2 u}{\partial y^2} \right) + 2 \left(\frac{\partial}{\partial x} \left(\nu_t \frac{\partial u}{\partial x} \right) \right) + \frac{\partial}{\partial y} \left(\nu_t \frac{\partial u}{\partial y} \right) \\ & + \frac{\partial}{\partial y} \left(\nu_t \frac{\partial u}{\partial x} \right) \end{aligned} \quad (2.2)$$

$$\begin{aligned} \frac{\partial v}{\partial t} + u \frac{\partial v}{\partial x} + v \frac{\partial v}{\partial y} = & -\frac{1}{\rho} \frac{\partial p}{\partial y} + \nu \left(\frac{\partial^2 v}{\partial x^2} + \frac{\partial^2 v}{\partial y^2} \right) + \left(\frac{\partial}{\partial x} \left(\nu_t \frac{\partial v}{\partial x} \right) + 2 \left(\frac{\partial}{\partial y} \left(\nu_t \frac{\partial v}{\partial y} \right) \right) \right) \\ & + \frac{\partial}{\partial x} \left(\nu_t \frac{\partial v}{\partial y} \right) \end{aligned} \quad (2.3)$$

$$\frac{\partial T}{\partial t} + u \frac{\partial T}{\partial x} + v \frac{\partial T}{\partial y} = \frac{\partial}{\partial x} \left(\left(\alpha + \frac{\nu_t}{Pr_t} \right) \frac{\partial T}{\partial x} \right) + \frac{\partial}{\partial y} \left(\left(\alpha + \frac{\nu_t}{Pr_t} \right) \frac{\partial T}{\partial y} \right) \quad (2.4)$$

$$\begin{aligned} \frac{\partial k}{\partial t} + u \frac{\partial k}{\partial x} + v \frac{\partial k}{\partial y} = & \frac{\partial}{\partial x} \left(\left(\alpha + \frac{\nu_t}{\sigma_k} \right) \frac{\partial k}{\partial x} \right) + \frac{\partial}{\partial y} \left(\left(\alpha + \frac{\nu_t}{\sigma_k} \right) \frac{\partial k}{\partial y} \right) - \epsilon \\ & + 2\nu_t \left(\frac{\partial u}{\partial x} \right)^2 + 2\nu_t \left(\frac{\partial v}{\partial y} \right)^2 + \nu_t \left(\frac{\partial u}{\partial y} + \frac{\partial v}{\partial x} \right)^2 \end{aligned} \quad (2.5)$$

$$\begin{aligned} \frac{\partial \epsilon}{\partial t} + u \frac{\partial \epsilon}{\partial x} + v \frac{\partial \epsilon}{\partial y} = & \frac{\partial}{\partial x} \left(\left(\nu + \frac{\nu_t}{\sigma_\epsilon} \right) \frac{\partial \epsilon}{\partial x} \right) + \frac{\partial}{\partial y} \left(\left(\nu + \frac{\nu_t}{\sigma_\epsilon} \right) \frac{\partial \epsilon}{\partial y} \right) - c_{2\epsilon} \frac{\epsilon^2}{k} \\ & + c_{1\epsilon} f_1 \left[2\nu_t \left(\frac{\partial u}{\partial x} \right)^2 + 2\nu_t \left(\frac{\partial v}{\partial y} \right)^2 + \nu_t \left(\frac{\partial u}{\partial y} + \frac{\partial v}{\partial x} \right)^2 \right] \end{aligned} \quad (2.6)$$

Where,

$$c_{1\epsilon} = 1.44 ; c_{2\epsilon} = 1.92 ; \nu_t = \frac{c_\mu k^2}{\epsilon} ; c_\mu = 0.09 ; \sigma_\epsilon = 1.3 ; \sigma_k = 1.0$$

2.2 Boundary conditions and Initial condition

Constant and Uniform velocity and temperature are given at inlet section of channel. Both left and right walls are given diabatic boundary condition of constant heat flux in the di-

rection normal to wall. No slip boundary condition is used at both walls. At outlet fully developed boundary condition is given for both velocity and temperature. Turbulent kinetic energy and dissipation at walls in the normal direction are also given equal to zero. The initial conditions for velocity and temperature are given as constant velocity and constant temperature equal to inlet conditions.

- Inlet:

$$u = u_i; v = 0; T = T_i$$

- Left and Right walls:

$$u = 0; v = 0; \frac{\partial T}{\partial y} = \left(-\frac{q_w}{\kappa}\right)$$

- Outlet:

$$\frac{\partial u}{\partial x} = 0; \frac{\partial T}{\partial x} = 0$$

- Initial conditions:

$$u = u_i; v = 0; T = T_i$$

2.3 Stream function and Vorticity formulation

Since the problem statement is two dimensional flow the continuity equation and momentum conservation equations can be converted into stream function (ψ) and vorticity (ω) transport equations.

$$\frac{\partial^2 \psi}{\partial x^2} + \frac{\partial^2 \psi}{\partial y^2} = -\omega \quad (2.7)$$

$$\frac{\partial \omega}{\partial t} + u \frac{\partial \omega}{\partial x} + v \frac{\partial \omega}{\partial y} = \nu \left\{ \frac{\partial^2 \omega}{\partial x^2} + \frac{\partial^2 \omega}{\partial y^2} \right\} \quad (2.8)$$

2.4 Non-dimensional form of GE

2.4.1 Non-dimensional variables

List of scales used for non-dimensional forms are

- Length scale - Channel width(h)
- Velocity scale - Inlet velocity(U_i)
- Temperature scale - Temperature using constant wall heat flux ($\frac{q_w h}{\kappa}$)

Using these scales remaining quantities are also converted to non-dimensional forms.

$$X = \frac{x}{h}; Y = \frac{y}{h}; U = \frac{u}{u_i}; V = \frac{v}{u_i}; \tau = \frac{tu_i}{h}$$

$$\theta = \frac{(T - T_i)}{\left(\frac{qw_h}{\kappa}\right)}; \Psi = \frac{\psi}{u_i h}; \Omega = \frac{\omega h}{u_i}; k_n = \frac{k}{u_i^2}; \epsilon_n = \frac{\epsilon h}{u_i^3}$$

2.4.2 Governing Equations

$$\frac{\partial^2 \Psi}{\partial X^2} + \frac{\partial^2 \Psi}{\partial Y^2} = -\Omega \quad (2.9)$$

$$\frac{\partial \Omega}{\partial \tau} + U \frac{\partial \Omega}{\partial X} + V \frac{\partial \Omega}{\partial Y} = \frac{1}{Re} \left(\frac{\partial^2}{\partial X^2} \left[\left(1 + \frac{\nu_t}{\nu} \right) \Omega \right] + \frac{\partial^2}{\partial Y^2} \left[\left(1 + \frac{\nu_t}{\nu} \right) \Omega \right] \right) + \frac{2}{\nu Re} \frac{\partial U}{\partial Y} \left(\frac{\partial^2 \nu_t}{\partial X^2} \right)$$

$$- \frac{2}{\nu Re} \frac{\partial V}{\partial X} \left(\frac{\partial^2 \nu_t}{\partial Y^2} \right) + \frac{2}{\nu Re} \left(\frac{\partial V}{\partial Y} - \frac{\partial V}{\partial X} \right) \left(\frac{\partial^2 \nu_t}{\partial X \partial Y} \right) \quad (2.10)$$

$$\frac{\partial \theta}{\partial \tau} + U \frac{\partial \theta}{\partial X} + V \frac{\partial \theta}{\partial Y} = \frac{\partial}{\partial X} \left(\left(\frac{1}{Pr} + \frac{\nu_t}{\nu Pr_t} \right) \frac{\partial \theta}{\partial X} \right) + \frac{\partial}{\partial Y} \left(\left(\frac{1}{Pr} + \frac{\nu_t}{\nu Pr_t} \right) \frac{\partial \theta}{\partial Y} \right) \quad (2.11)$$

$$\frac{\partial k_n}{\partial \tau} + U \frac{\partial k_n}{\partial X} + V \frac{\partial k_n}{\partial Y} = \frac{1}{Re} \left\{ \frac{\partial}{\partial X} \left(\left(1 + \frac{\nu_t}{\nu \sigma_k} \right) \frac{\partial k_n}{\partial X} \right) + \frac{\partial}{\partial Y} \left(\left(1 + \frac{\nu_t}{\nu \sigma_k} \right) \frac{\partial k_n}{\partial Y} \right) \right\}$$

$$- \epsilon_n + \frac{\nu_t}{\nu Re} \left[2 \left(\frac{\partial U}{\partial X} \right)^2 + 2 \left(\frac{\partial V}{\partial Y} \right)^2 + \left(\frac{\partial U}{\partial Y} + \frac{\partial V}{\partial X} \right)^2 \right] \quad (2.12)$$

$$\frac{\partial \epsilon_n}{\partial \tau} + U \frac{\partial \epsilon_n}{\partial X} + V \frac{\partial \epsilon_n}{\partial Y} = \frac{1}{Re} \left[\frac{\partial}{\partial X} \left(\left(1 + \frac{\nu_t}{\nu \sigma_\epsilon} \right) \frac{\partial \epsilon_n}{\partial X} \right) + \frac{\partial}{\partial Y} \left(\left(1 + \frac{\nu_t}{\nu \sigma_\epsilon} \right) \frac{\partial \epsilon_n}{\partial Y} \right) \right]$$

$$- c_{2\epsilon} \frac{\epsilon_n^2}{k_n} + \frac{c_{1\epsilon} f_1 \nu_t}{Re \nu} \left[2 \left(\frac{\partial U}{\partial X} \right)^2 + 2 \left(\frac{\partial V}{\partial Y} \right)^2 + \left(\frac{\partial U}{\partial Y} + \frac{\partial V}{\partial X} \right)^2 \right] \quad (2.13)$$

2.5 Non-dimensional Boundary conditions and Initial Condition

- Inlet: For k_n and ϵ_n , 7% turbulent intensity is given at inlet.

$$U = 1, \quad V = 0, \quad \theta = 0, \quad \frac{\partial \Psi}{\partial Y} = 1, \quad I = \sqrt{\frac{2k_n}{3U}}; \quad \frac{\nu_t}{\nu} = 10;$$

- Left and Right walls:

$$U = 0, \quad V = 0, \quad \frac{\partial \theta}{\partial Y} = -1, \quad \Psi = 0, \quad \Omega = -\frac{\partial^2 \Psi}{\partial Y^2}$$

- Outlet: Fully developed boundary condition is applied.

$$\frac{\partial \theta}{\partial Y} = 0, \quad \Omega = -\frac{\partial^2 \Psi}{\partial Y^2}$$

- Initial condition:

$$U = 1, \quad V = 0, \quad \theta = 0$$

Chapter 3

Numerical methods

Finite difference method is used to discretize the governing equations. The discretized governing equations are applied at the nodal points of the discretized grid. The solver that is used to develop the code for solving these governing equations is FORTRAN 90. The Stream function equation (*SFE*) is discretized using second order central difference scheme CD_2 . Bi-conjugate gradient method is used to solve *SFE*. Diffusion terms in Vorticity transport equation (*VTE*), Energy equation (*EE*), Kinetic energy and dissipation equations are also discretized using central difference scheme. Temporal derivatives are solved explicitly using fourth order Range-kutta (*RK4*) scheme. Compact schemes^[26, 27] are used to discretize the non-linear convective terms. To avoid numerical instability a small non-dimensional time step of 10^{-4} is used to solve the equations.

Table 3.1: *Numerical methods used for simulation*

Equation	Numerical method
Governing equations	Finite difference method
Stream function equations	CD_2 , Bi-conjugate gradient method
Diffusion terms	Central difference scheme
Convective terms	Compact scheme
Temporal term	Range-Kutta 4 th order explicit

Chapter 4

Results and Discussion

The turbulent forced convection flow through a channel is numerically studied and the heat transfer characteristics are reported for low Prandtl number fluids. The vertical channel has height to width aspect ratio of 10.0. Uniform heat flux is applied at the channel walls. The prominent liquid metals that are used in nuclear applications are sodiumpotassium (NaK), mercury, LBE and sodium. The molecular Prandtl number of NaK, Mercury and LBE are close to each other, i.e. in the range of 0.01 – 0.03, whereas the Prandtl number of sodium is smaller, about 0.006. In the present study heat transfer characteristics are reported using Pr values equal to 0.01 and 0.025.

4.1 Grid independence and Validation

The grid independence test has been conducted using three grid sizes of 400 x 60, 600 x 80, 800 x 100, at $Re=8000$, $Pr=0.01$ and $Pr_t=6$. The velocity and temperature profiles at the outlet of the channel are plotted with different grids and shown in Fig. 4.1. The velocity and temperature profiles are shown grid independence with grid size of 600x80. Hence all simulations are reported with grid size of 600 x 80.

Figure 4.1: Grid independence for velocity and temperature profiles at $Re=8000, Pr=0.01$

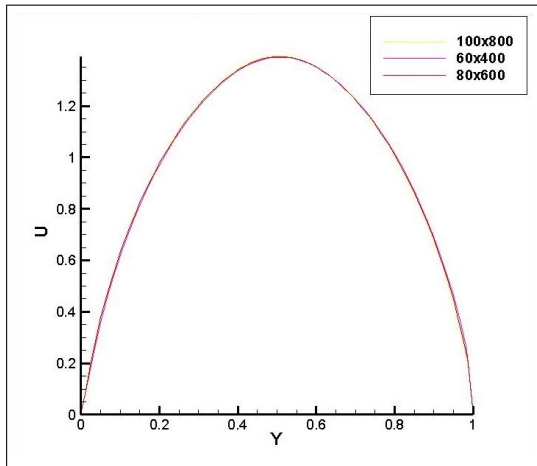


Figure 4.2: U - grid independence

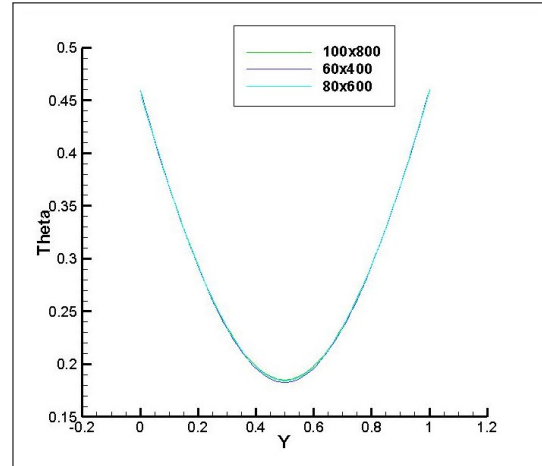


Figure 4.3: θ - grid independence

Validation of *RANS* code with standard $k-\epsilon$ model is done comparing with *DNS* and *LES* simulation from Duponcheel.et.al^[25] at $Pr=0.01$ with Reynolds numbers 5600, 22000, 87000. Friction temperature (T_τ) and friction velocity (u_τ) are used in the above paper and hence the results are converted in terms of non-dimensional friction temperature (θ^+) and non-dimensional length scale (Y^+) and plotted as shown in Fig. 4.4. y^+ is non-dimensional y co-ordinate with length scale using kinematic viscosity(ν) and friction temperature (u_τ) and shown in Eq.4.1. Friction temperature is the temperature obtained using wall heat flux(q_w) and friction velocity (u_τ). At $Re=5600$ using different turbulent Prandtl numbers ranging from 4.12 to 7 numerical simulations are performed and temperature profile at the outlet of the channel is plotted and shown in Fig.4.5. The temperature profile from *RANS* approach is matching well with the *DNS* result both in near wall region and also in the center of channel. At $Re=22000$ numerical simulations are performed and temperature profile is shown in Fig.4.6 at turbulent Prandtl numbers ranging from 9 to 13. The temperature profile from *RANS* approach is matching with the *LES* result near the wall region.

Figure 4.4: Validation of temperature profile in the channel with DNS and LES profiles

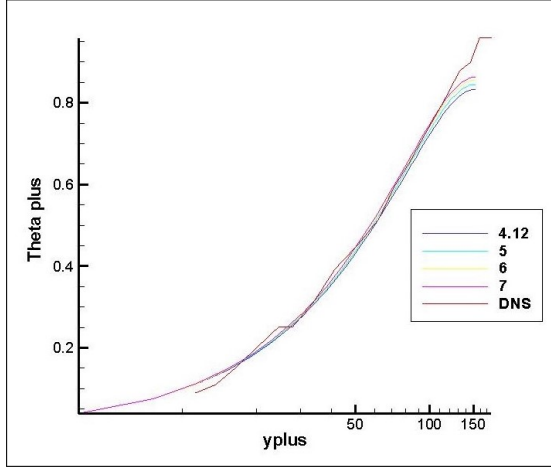


Figure 4.5: $Re=5600, Pr=0.01$

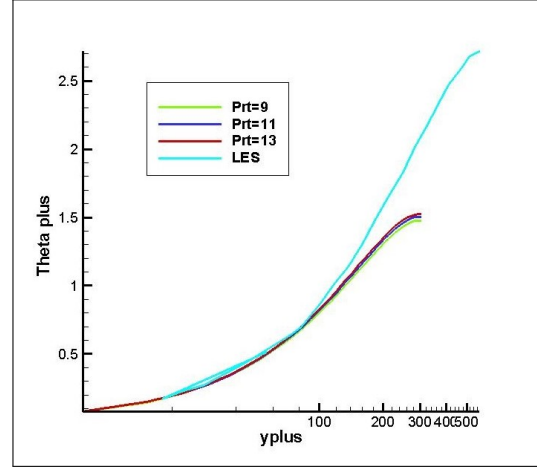


Figure 4.6: $Re=22000, Pr=0.01$

$$\theta^+ = \left(\frac{T_w - T}{T_\tau} \right); T_\tau = \frac{q_w}{(\rho C_p u_\tau)}; u_\tau = \sqrt{\nu \left(\frac{\partial U}{\partial Y} \right)_{wall}}; y^+ = \frac{y}{\left(\frac{\nu}{u_\tau} \right)} \quad (4.1)$$

4.2 Effect of Reynolds number

The effect of Reynolds number is presented by using results at Re equal to 5600, 8000, 22000, 87000 at $Pr=0.01$. U velocity contour plots at these Reynolds numbers are shown in the Fig.4.7. At each of these Re the flow is fully developed and it occurs around non-dimensional length of $X=4$. The dimensional velocity increases with increase in Re but dimensionless velocity is not changing because the velocity scale used for non-dimensionalisation is inlet velocity. Hence all the U contour plots look alike. Temperature contour plots using the non-dimensional temperature (θ^+) are shown in the Fig.4.8. (θ^+) is fully developed at all the presented Re . For $Re=5600$ and $Re=8000$ θ^+ is fully developed around $X=2$ whereas for $Re=22000$ θ^+ is fully developed around $X=3$. For $Re=87000$ θ^+ is fully developed around $X=4$. As Re increases the length required for the temperature to be fully developed increases. The steady state velocity and temperature profiles at the outlet of channel where the flow is fully developed are shown in Fig. 4.11. The U velocity profile for different Re is same and shown in the Fig.4.9. U velocity has a maximum value of 1.3 at the centre of the channel and a minimum value of zero at

channel walls. The non-dimensional temperature (θ) profile at the outlet for different Re is shown in the Fig.4.10. As Re increases, using the same fluid, inlet velocity increases and hence the velocity in the channel also increases. As the Re increases the turbulence intensity increases and the energy of fluctuating component increases. Hence the mean temperature at constant heat flux decreases. Thus the temperature (θ) decreases with increase in Re due to increase in velocity of the fluid. At any particular Re , θ is maximum at wall, due to the boundary condition of constant heat flux, and decreases towards the center of the channel ($Y=0.5$).

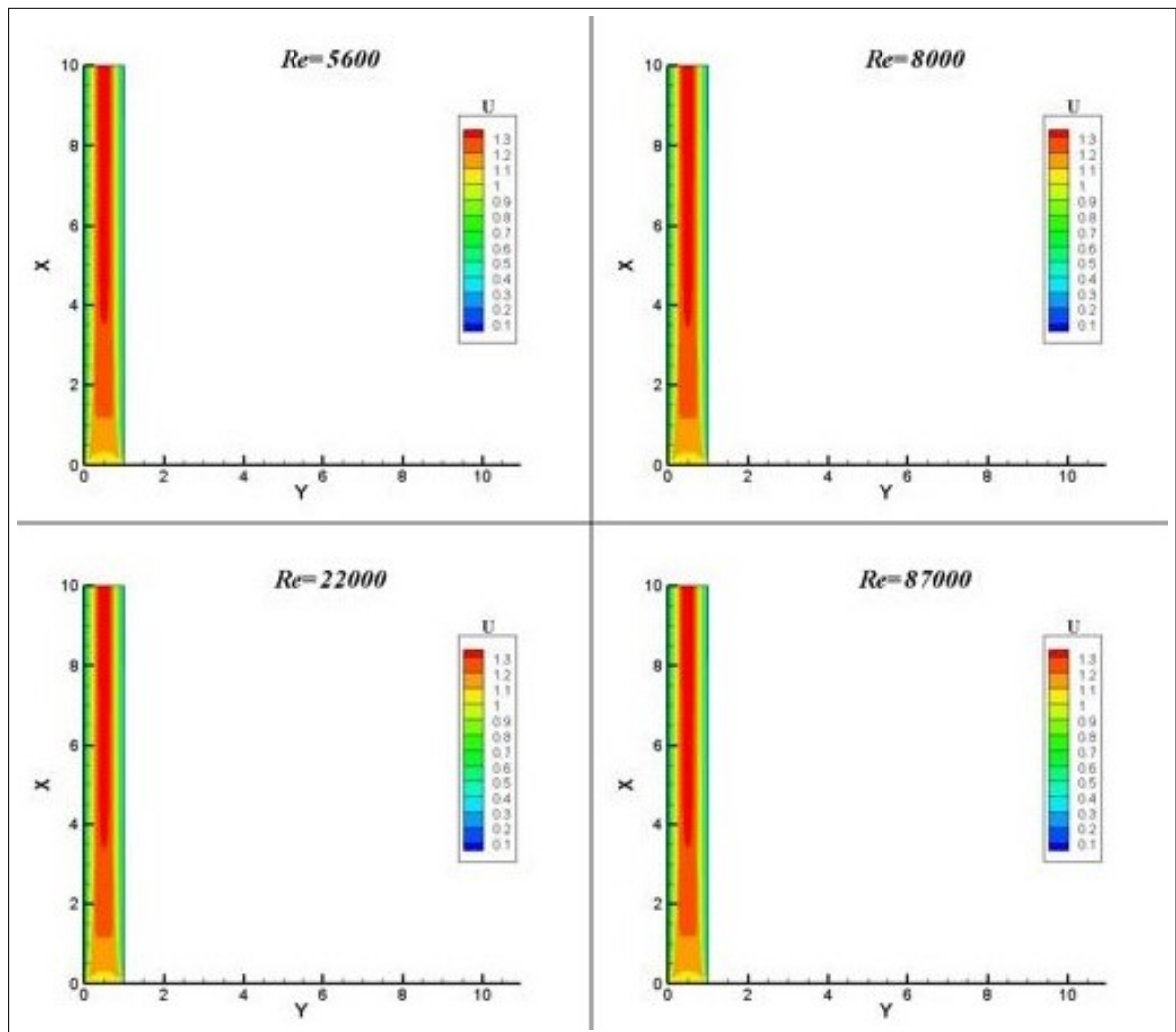


Figure 4.7: Contour plots of effect of Re on Velocity(U) at a cross-section of channel

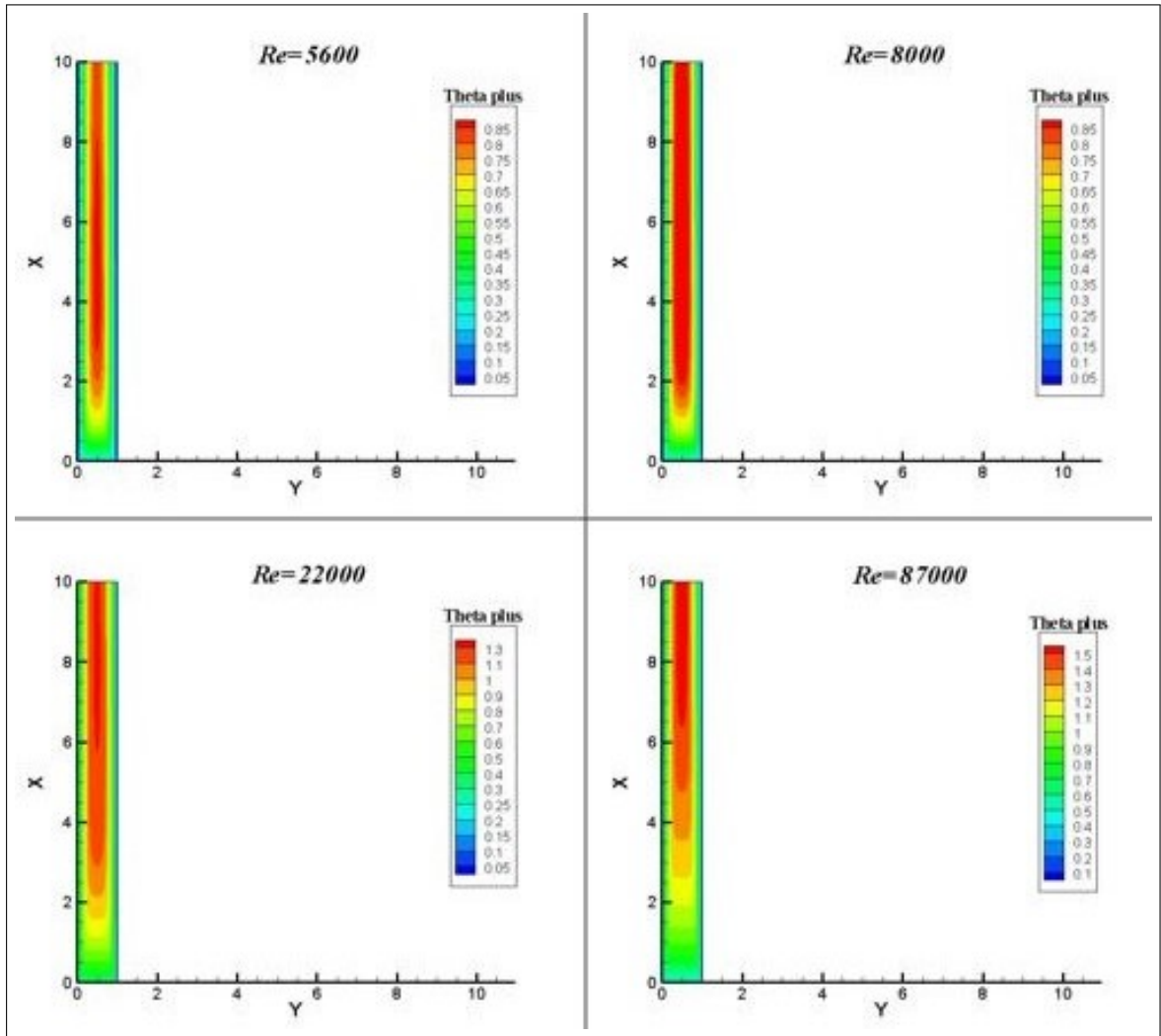


Figure 4.8: Contour plots of effect of Re on friction temperature (θ^+) at a cross-section of channel

Figure 4.9: Effect of Re on U

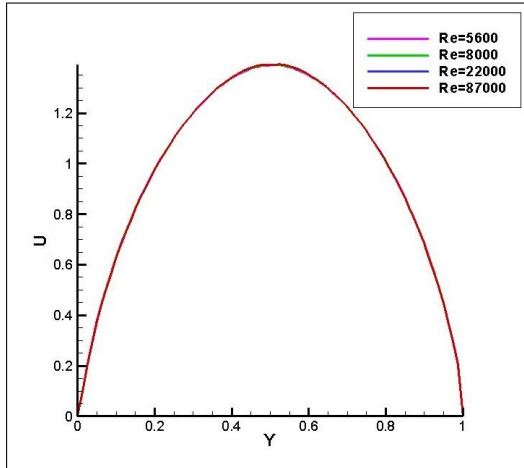


Figure 4.10: Effect of Re on θ

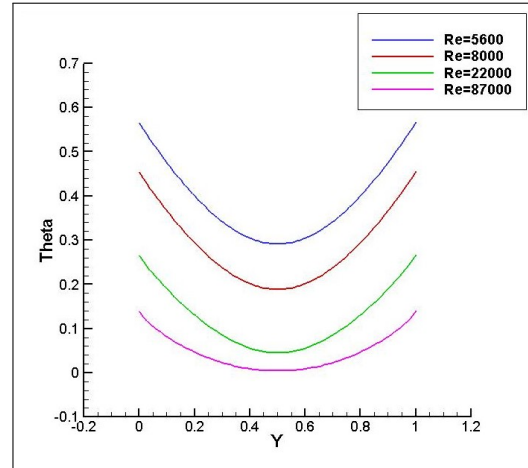


Figure 4.11: Effect of Re on velocity and temperature profiles at outlet of the channel at $Pr=0.01$

4.3 Effect of Prandtl number

The effect of Pr on temperature is presented using Pr equal to 0.01 and 0.025 at Re equal to 8000 and Pr_t equal to 4.12. Contour plots of temperature (θ^+) at both Pr are shown in the Fig.4.13. For $Pr=0.01$ θ^+ is fully developed around $X=3$ where as for $Pr=0.025$ θ^+ is fully developed around $X=5$. Hence as Pr increases the length required for temperature profile to be fully developed increases. As momentum diffusivity increases the turbulent component increases in the flow and less are the mean components at particular Reynolds number. As thermal diffusivity decreases the more are the mean components of temperature. The combined effect is presented in the non-dimensional number Pr . Hence as Pr increases mean components of temperature decreases and it can be seen from Fig. 4.12. For $Pr=0.01$ θ has a maximum value of 0.45 at channel walls and minimum value of 0.2 at the center of the channel where as for $Pr=0.025$ θ has a maximum value of 0.26 at channel walls and minimum value of 0.05 at center of the channel. Since the constant heat flux boundary condition is applied at walls, as Pr increases at a particular Re both the wall temperatures ($\theta(Y = 0)$ & $\theta(Y = 1)$) and the mean temperature (θ_{mean}) at a cross-section of channel in fully developed region decreases.

Figure 4.12: Effect of Pr on temperature at a cross-section of channel

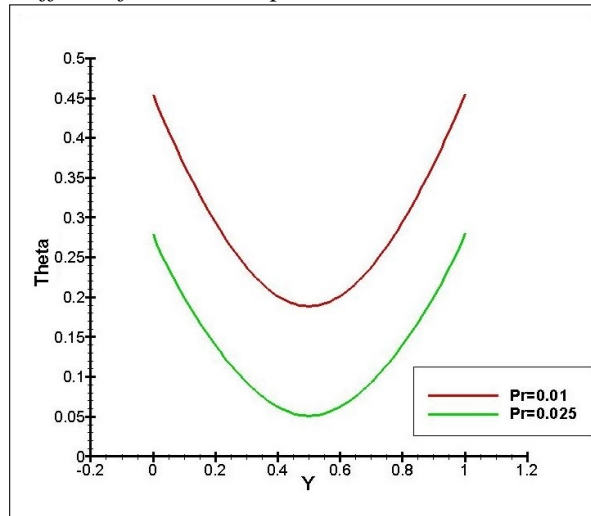
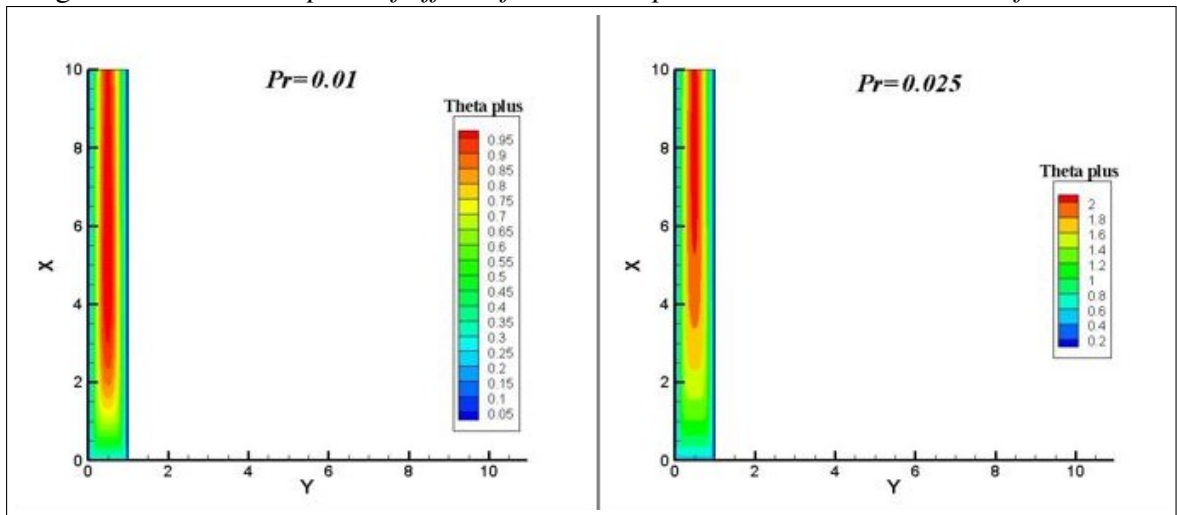


Figure 4.13: Contour plots of effect of Pr on temperature at a cross-section of channel



4.4 Effect of Turbulent Prandtl number

The effect of Pr_t on temperature is presented using Pr_t equal to 4.12, 5, 6, 7 at $Re=8000$ using Pr equal to 0.01. Pr_t is defined as the ratio of eddy kinematic diffusivity to eddy thermal diffusivity. Hence the effects of both eddy diffusivities are included in Pr_t . In *RANS* approach from boussinesq approximation temperature fluctuating components are modeled as the product of eddy thermal diffusivity and gradient of mean temperature. At constant Re and Pr the turbulent intensity remains constant and fluctuating components remain constant. Hence as Pr_t increases the eddy thermal diffusivity decreases. As eddy

thermal diffusivity decreases the gradient of mean temperature increases at any particular section of channel in the fully developed region. Contour plots of non-dimensional temperature (θ) at different Pr_t is shown in the Fig. 4.15. From that figure as Pr_t increases the gradients of mean temperature (θ) increases and thus the temperature difference between the wall and fluid at center of channel increases. As Pr_t increases the θ at center of channel decreases and θ at wall increases at constant Re and Pr under same boundary conditions. It can be observed from the temperature (θ) profile at channel section as shown in Fig. 4.14.

Figure 4.14: *Effect of Pr_t on temperature at a cross-section of channel*

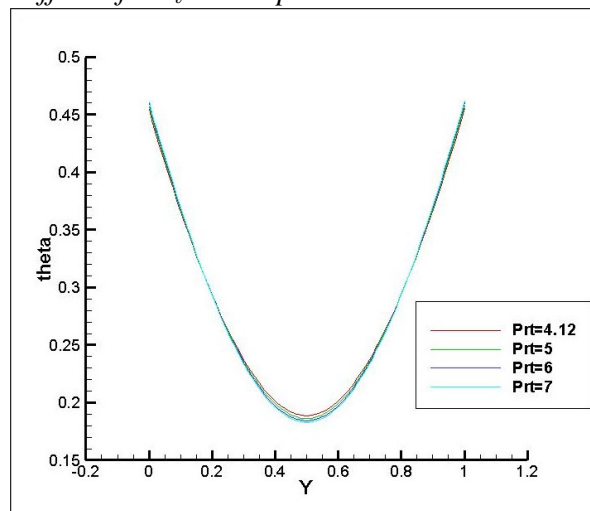
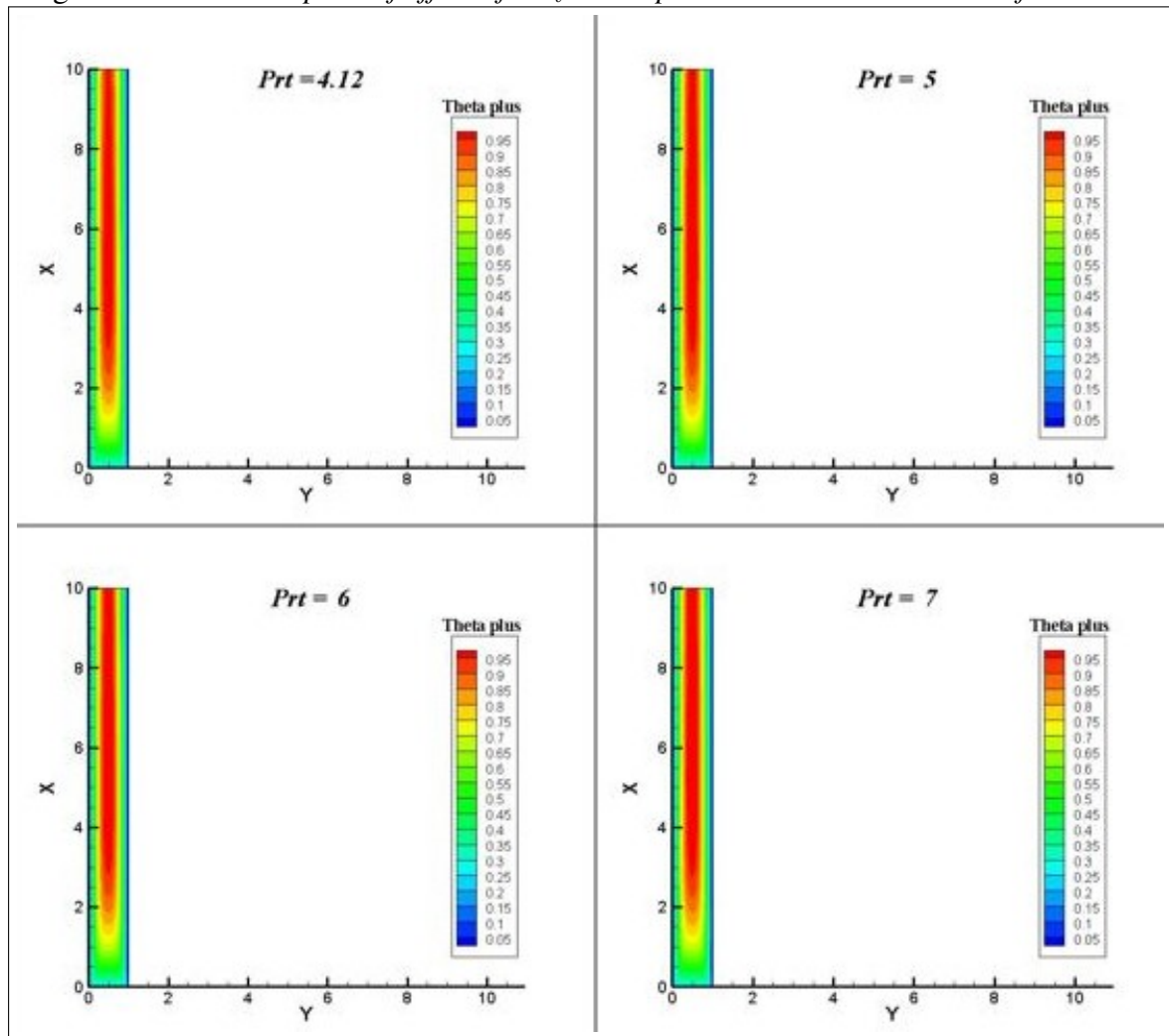


Figure 4.15: Contour plots of effect of Pr_t on temperature at a cross-section of channel



4.5 Nusselt number (Nu) calculation

The overall heat transfer is characterized by bulk Nusselt number (Nu) and it is calculated as

$$Nu = \int Nu_{local} dX = \int \frac{1}{(\theta_{wall} - \theta_{mean})} dX$$

$$\theta_{mean} = \frac{1}{Y U_{mean}} \int (U\theta) dY$$

$$U_{mean} = \frac{1}{Y} \int U dY$$

Where,

θ_{mean} = Mean temperature at a section in the channel.

U_{mean} = Mean velocity at a section in the channel.

Simpson's $\frac{1}{3}$ rule is used for the numerical integration.

4.6 Effect of Re on Nu

Nusselt number Nu is the ratio of convective heat transfer to the conductive heat transfer in the fluid flow. As the Re increases the velocity of fluid in the channel increases and hence the convective heat transfer in the fluid flow increases and thus the Nu increases. As Re increases also the mean temperature at a cross-section of the channel and the wall temperature decreases under the constant heat flux boundary conditions using the same fluid but the difference between the wall temperature (θ_w) and mean temperature (θ_{mean}) at a channel cross-section increases as shown in Fig.4.10. Since the local Nusselt number (Nu_{local}) is the inverse of $(\theta_w - \theta_{mean})$ it increases and hence the bulk Nusselt number Nu increases. Effect of Re on Nu is shown using the Table 4.1, at $Pr_t = 5$, and fluid is having $Pr = 0.01$.

Table 4.1: Effect of Re on Nu at $Pr = 0.01$

Reynolds number (Re)	Nusselt number (Nu)
5600	4.92
8000	5.09
22000	6.13
87000	9.61

4.7 Effect of Pr on Nu

Pr is the ratio of momentum diffusivity (ν) to thermal diffusivity (α) and it can be increased either by increasing the momentum diffusivity (ν) or by decreasing the thermal diffusivity (α). As ν increases at constant Re the velocity of the fluid decreases and hence the convective heat transfer decreases. Thus as ν increases Nu decreases at constant Re . As α decreases at constant Re the temperature gradients in Y-direction increases and thus the fluctuating components of temperature increases and hence mean temperature component decreases. Therefore the mean temperature at a cross-section of channel

decreases and also the wall temperature decreases but their difference increases and shown in the Fig.4.12. Thus the local Nu_{local} and Nu decreases with decrease in α . Now the combined effect of ν and α is given by Pr . As the Pr increases the increase in Nu due to increase in ν is more compared to decrease in Nu due to decrease in α , under the same boundary conditions and at same Re . Hence the Nu increases as Pr increases. It can be shown using the Table 4.2 in which $Re=8000$, $Pr_t=5$.

Table 4.2: *Effect of Pr on Nu*

Prandtl number (Pr)	Nusselt number (Nu)
0.01	5.09
0.025	5.98

4.8 Effect of Pr_t on Nu

Pr_t is the ratio of eddy momentum diffusivity (ν_t) to eddy thermal diffusivity (α_t). Pr_t can be increased either by increasing the ν_t or by decreasing the α_t . As ν_t increases at constant Re and Pr the gradient of mean component of velocity decreases and thus the momentum is transferred away from the wall and thus the convective heat transfer from the wall to fluid increases. Hence as ν_t increases the Nu increases at constant Re and Pr . As α_t decreases the gradients of mean component of temperature increases and thus the thermal energy is less diffused from wall. Hence as α_t decreases the Nu decreases. Now the combined effect of both ν_t & α_t is given by Pr_t . As Pr_t increases the increase in Nu due to increase in ν_t is less than the decrease in Nu due to decrease in α_t , for $Pr_t > 1$. Hence as Pr_t increases the Nu decreases. Also as the Pr_t increases the mean temperature over the section of the channel increases under the same boundary conditions and using the same fluid at constant Re . It can be seen in the Table 4.3 which is computed using $Re=8000$, $Pr=0.01$ that as Pr_t increases Nu decreases.

Table 4.3: *Effect of Pr_t on Nu*

Turbulent Prandtl number (Prt)	Nusselt number (Nu)
4.12	5.17
5	5.09
6	5.03
7	4.98

Table 4.4: Effect of Pr_t on Nu at $Pr=0.01$

Reynolds Number (Re)	Turbulent Prandtl number (Prt)	Nu from RANS approach	Nu from Cheng and Tak correlation
5600	4.12	4.97	4.95
	5	4.92	
	6	4.87	
	7	4.84	
8000	4.12	5.17	5.09
	5	5.09	
	6	5.03	
	7	4.98	
22000	4.12	6.29	5.84
	5	6.13	
	6	6	
	7	5.9	
	9	5.77	
	11	5.68	
	13	5.62	
87000	4.12	9.89	8.54
	5	9.61	
	6	9.36	
	7	9.16	
	10	8.76	
	13	8.5	
	16	8.33	

4.9 Correlation developed for Pr_t

The correlation that is proposed by Cheng and Tak^[12] for Nu is

$$Nu = A + 0.018Pe^{0.8}$$

where, $A = 4.5$ $Pe \leq 1000$
 $= 5.4 - (9Pe * 10^{-4})$ $1000 \leq Pe \leq 2000$
 $= 3.6$ $Pe \geq 2000$

Comparison of RANS simulated Nu results with Cheng and Tak Nu is presented in the Table 4.4 at $Pr=0.01$ and in the Table 4.5 at $Pr=0.025$.

Table 4.5: Effect of Pr_t on Nu at $Pr=0.025$

Reynolds Number (Re)	Turbulent Prandtl number(Pr_t)	Nu from $RANS$ approach	Nu from Cheng and Tak correlation
5600	4.12	5.66	5.43
	5	5.54	
	6	5.44	
	7	5.37	
8000	4.12	6.14	5.74
	5	5.98	
	6	5.86	
	7	5.77	
22000	4.12	8.43	7.3
	5	8.17	
	6	7.95	
	7	7.78	
	9	7.54	
	11	7.38	
	13	7.26	
87000	4.12	13.42	12.02
	5	12.99	
	6	12.79	
	7	12.61	
	10	12.18	
	13	11.85	
	16	11.59	

Using the data from Table 4.4 and Table 4.5 at each Peclet number(Pe) curve fitting technique is used between the turbulent Prandtl number and Nu obtained from $RANS$ approach to acquire the Pr_t for which the Nu obtained from $RANS$ approach matches with that of Nu from Cheng and Tak. Using the Pr_t data obtained at each Pe a correlation is developed for Pr_t as a function of Pe and shown in the Eq.4.2

$$\begin{aligned}
 Pr_t &= 0.9719Pe^{0.3796} & 56 \leq Pe \leq 220 \\
 &= 4.903 + 0.0138Pe - (5Pe^2 * 10^{-6}) & 220 \leq Pe \leq 2175 \quad (4.2)
 \end{aligned}$$

Chapter 5

Conclusions

Heat transfer characteristics of turbulent forced convection in the channel flow at low Prandtl number are studied numerically using *RANS* approach. The following conclusions are drawn from present study

- As the Reynolds number increases the temperatures both at wall and center of channel decreases and thus the mean temperature at a section of channel also decreases at constant heat flux boundary condition and constant Prandtl number.
- As the Prandtl number increases the temperatures both at wall and center of channel decreases and thus the mean temperature at a section of channel also decreases at constant heat flux boundary condition and constant Reynolds number.
- As the Reynolds number increases the mean temperature at any section of channel decreases thus overall Nusselt number increases due to increase of velocity of fluid.
- As the Prandtl number increases the mean temperature at any section of channel decreases and thus overall Nusselt number increases at constant Reynolds number.
- A parametric study on turbulent Prandtl number is done and found that as Pr_t increases the temperature at wall increases and the temperature at center of channel decreases, but the mean temperature at any section of channel increases. Thus as Pr_t increases Nusselt number of channel decreases.
- Using above parametric study and comparing Nusselt number with correlation given by Xeng and Tak a new correlation for Pr_t is developed for validity range of Peclet number(Pe) from 56 to 2175.
- Present results can be used for understanding the heat transfer characteristics of liquid metal flows in nuclear applications.

References

- [1] S. David. Future Scenarios for Fission Based Reactors. *Nuclear Physics A* 751, (2005) 419–441.
- [2] J. Benemann. Status Report on Solar Through Power Plants. *Pilkington Press* .
- [3] OECD, NEA, and N. S. Committee. Handbook on Lead-bismuth Eutectic Alloy and Lead Properties, Materials Compatibility, Thermal-hydraulics and Technologies. Nuclear Science, 2007.
- [4] W. Beitz and K. H. Kttner. *Dubbel-Taschenbuch des Maschinenbaus*. 15th edition. Springer-Verlag, 1986.
- [5] P. L. Kirillov. Generalization of experimental data on heat transfer in molten metals. *Atom. Energy* 13(1), (1963) 1103–1106.
- [6] C. A. Sleicher, A. S. Awad, and R. H. Notter. Temperature and Eddy diffusivity profiles in NaK. *Int. J. Heat Mass Transfer* 16, (1973) 1565–1575.
- [7] E. Skupinski, J. Tortel, and L. Vautrety. Tetermination des coefficients de convection Dun Alliage sodiumpotassium Dans un Tube Circulaire. *Int. J. Heat Mass Transfer* 8, (1965) 937–951.
- [8] W. K. Stromquist. Effect of wetting on heat transfer characteristics of liquid metals. *University of Tennessee ORO-63*.
- [9] H. Kawamura, K. Ohsaka, H. Abe, and K. Yamamoto. DNS Of Turbulent Heat Transfer In Channel Flow With Low To Medium-high Prandtl Number Fluid. *International Journal Of Heat And Fluid Flow* 19, (1998) 482–491.
- [10] H. Kawamura, H. Abe, and Y. Matsuo. DNS Of Turbulent Heat Transfer in Channel flow with respect to Reynolds and Prandtl number effects. *International Journal Of Heat And Fluid Flow* 20, (1999) 196–207.

- [11] A. J. Reynolds. The Prediction Of Turbulent Prandtl And Schmidt Numbers. *Int. J. Heat Mass Transfer* 18, (1975) 1055–1069.
- [12] X. Cheng and N. Tak. Investigation on turbulent heat transfer to leadbismuth eutectic flows in circular tubes for nuclear applications. *Nuclear Engineering And Design* 236, (2006) 385–393.
- [13] S. Aoki. A consideration on the heat transfer in liquid metal. *Bull. Tokyo Inst. Tech.* 54, (1963) 63–73.
- [14] O. E. Dwyer. Recent developments in liquid metal heat transfer. *Atom. Energy Rev.* 4(1), (1966) 3–92.
- [15] R. C. Martinelli. Heat transfer to molten metals. *Trans. ASME* 69, (1947) 47–59.
- [16] R. N. Lyon. Liquid metal heat transfer coefficients. *Chem. Eng. Progr.* 47, (1951) 75–79.
- [17] M. Ibragimov, V. I. Subbotin, and P. A. Ushakov. Investigation of heat transfer in the turbulent flow of liquid metals in tubes. *Atomnaya Energiya* 8(1), (1960) 54–56.
- [18] P. L. Kirillov and P. A. Ushakov. Heat transfer to liquid metals: specific features, methods of investigation, and main relationships. *Thermal Eng.* 48(1), (2001) 50–59.
- [19] H. A. Johnson, J. P. Hartnett, and W. J. Clabaugh. Heat transfer to molten leadbismuth eutectic in turbulent pipe flow. *J. Heat Transfer* 75, (1953) 1191–1198.
- [20] P. L. Kirillov. The summary of experimental data on heat transfer in liquid metals. *Atomnaya Energiya* 13, (1962) 481–484.
- [21] V. I. Subbotin, M. K. Ibragimov, M. N. Ivanovsky, M. N. Arnoldov, and E. V. Nomofilov. Turbulent heat transfer in a flow of liquid metals. *Int. J. Heat Mass Transfer* 4, (1961) 79–87.
- [22] T. Abram and S. Ion. Generation-IV Nuclear Power: A Review Of The State Of The Science. *Energy Policy* 36, (2008) 4323–4330.
- [23] L. Bricteuxa, M. Duponcheela, G. Winckelmansa, I. Tiselj, and Y. Bartosiewiczza. Direct And Large Eddy Simulation Of Turbulent Heat Transfer At Very Low Prandtl Number: Application To Leadbismuth Flows. *Nuclear Engineering And Design* 246, (2012) 91–97.

- [24] W. M. Kays. Turbulent Prandtl Number where Are We. *J. Heat Transfer* 116, (1994) 284–295.
- [25] M. Duponcheel, L. Bricteux, M. Manconi, G. Winckelmans, and Y. Bartosiewicz. Assessment of RANS and improved near-wall modeling for forced convection at low Prandtl numbers based on LES up to $Re_\tau=2000$. *International Journal of Heat and Mass Transfer* 75, (2014) 470–482.
- [26] T. K. Sengupta, S. K. Sirkar, and A. Dipankar. High accuracy schemes for DNS and acoustics. *J. Sci. Comput.* 26, (2006) 151–193.
- [27] K. Venkatasubbaiah and T. K. Sengupta. Mixed convection flow past a vertical plate: Stability analysis and its direct simulation. *Int. J. Therm. Sci.* 48, (2009) 461–474.